LegoBot: Modular, Compact, Device-Agnostic Robot for Endovascular Catheter and Guidewire Manipulation in Stroke Thrombectomy

Weibo Gao, *Graduate Student Member, IEEE*, Nitin Srinivasan, Dongming Piao, Qianhe Fan, Miki Guo, Rui Li, Peter Patalano, and Hao Su, *Senior Member, IEEE*

***Abstract*—State-of-the-art endovascular robots are often limited by coupled translation–rotation actuation, narrow compatibility with off-the-shelf devices, and fixed architectures that are difficult to reconfigure for multidevice procedures. These limitations are especially restrictive in neurovascular intervention, where long working lengths, tortuous anatomy, and coordinated manipulation of multiple catheters and guidewires are frequently required. In this work, we present LegoBot, a modular, compact, device-agnostic robot for neurovascular catheter and guidewire manipulation. First, we design a decoupled two-degree-of-freedom (2-DOF) actuation mechanism together with an instrument-agnostic adjustable clamping mechanism, enabling independent or simultaneous instrument translation and rotation while accommodating off-the-shelf devices with diameters ranging from 0.33 to 3 mm. Second, we present the mechatronic design of a modular catheter robot with interchangeable adapters for different instruments, which support module-level device exchange. We also design a module coupler that connects adjacent robotic modules for multi-instrument actuation and improves rotational torque transmission through long, compliant instruments. Benchtop characterization of the proposed 2-DOF mechanism showed peak insertion force up to 5.3 N and rotational torque up to 8.4 mN·m, exceeding reported clinical requirements. Phantom studies demonstrated a two-module (4-DOF) configuration for diagnostic angiography and a three-module (6-DOF) configuration for aspiration thrombectomy, including successful clot aspiration in a neurovascular phantom.**

***Index Terms*—Endovascular robots, medical robots, modular, neurovascular intervention, thrombectomy.**

I. Introduction

ENDOVASCULAR interventions, such as diagnostic angiography and stroke thrombectomy, require precise manipulation of long, flexible guidewires and catheters through tortuous vasculature under fluoroscopic guidance. These procedures remain heavily skill-dependent and physically demanding, with performance sensitive to operator dexterity, fatigue, and repeated instrument handling [1]. Robotic-assisted intervention has the potential to improve motion consistency and ergonomics [2], [3], and reduce the clinicians' radiation exposure [4], but still faces challenges in preserving compatibility with standard clinical devices and workflows.

Among endovascular procedures, neurovascular intervention imposes some of the most challenging mechatronic requirements. Intracranial navigation involves long working lengths, tortuous and fragile anatomy, and coordinated use of multiple slender devices. Diagnostic angiography typically requires coordinated advancement and axial rotation of a guidewire and catheter to reach intracranial targets and deliver contrast. Aspiration thrombectomy is even more demanding, often requiring controlled manipulation of a biaxial or triaxial instrument stack together with standard accessory connections for contrast injection and aspiration [5], [6], [7]. We target neurovascular intervention as the focus of this work (see Fig. 1), while the mechatronic design principles are relevant more broadly to other endovascular procedures.

State-of-the-art robotic systems have demonstrated the potential of robotic assistance for endovascular intervention. Siemens Corindus provides precise teleoperation from a radiation-shielded cockpit but is built as a largely fixed platform and typically requires manual interruption for multidevice exchange [8]. LIBERTY eliminates heavy capital equipment through a disposable, partially modular design yet actuates only guidewires and microcatheters with a total of three degrees of freedom (DOFs), mainly targeting peripheral intervention [9], [10]. Magellan

Received 14 January 2026; revised 30 March 2026; accepted 12 May 2026. Recommended by Technical Editor W. Li and Senior Editor Z. Sun. This work was supported in part by the NIH under Grant 1R01NS141171-01, in part by the NSF CPS under Grant 2344956, in part by the NSF GCR under Grant 2524088, and in part by the NYU MEGA-Grants Initiative Fund under Grant A25-0942-001. *(Corresponding author: Hao Su.)*

Weibo Gao, Nitin Srinivasan, Dongming Piao, Qianhe Fan, Miki Guo, and Rui Li are with the Lab of Biomechatronics and Intelligent Robotics, Department of Biomedical Engineering, New York University, New York, NY 11201 USA.

Peter Patalano is with the Department of Surgery, NYU Grossman School of Medicine, New York, NY 10016 USA.

Hao Su is with the Lab of Biomechatronics and Intelligent Robotics, Department of Biomedical Engineering, New York University, New York, NY 11201 USA, and also with the Department of Computer Science, Courant Institute School of Mathematics, Computing, and Data Science, New York University, New York, NY 10012 USA (e-mail: hao.su@nyu.edu).

This article has supplementary material provided by the authors and color versions of one or more figures available at https://doi.org/10.1109/TMECH.2026.3695773.

Digital Object Identifier 10.1109/TMECH.2026.3695773

TABLE I
COMPARISON OF STATE-OF-THE-ART CATHETER ROBOTS AND THE PROPOSED MODULAR CATHETER ROBOT

Characteristics	Siemens Corindus CorPath GRX [17]	Microbot LIBERTY [9]	Magellan [18]	Robocath R-One [12]	ICL [13]	KAIST [14]	BIT [15]	Our previous work [16]	Proposed modular catheter robot (this work)
Off-the-shelf instruments agnostic	No	Yes	No	No	Yes	No	Yes	Yes	Yes
Mechanism-level decoupled translation and rotation DOFs	No	No	N.R.	Yes	No	No	No, coupled catheter T/R	No, coupled guidewire T/R	Yes
Modularity	Not modular	Partially modular, disposable robot	Not modular	Not modular	Not modular	Partially modular	Partially modular	Partially modular	Fully modular, enables module-level device exchange
DOF 1: guidewire translation	Continuous*	Continuous*	Continuous*	Continuous*	Extended via regripping (SSL 20 mm)	N.S.	Extended via regripping (SSL N.R.)	Continuous*	Continuous*
DOF 2: guidewire rotation	$\pm 180^\circ$	$\pm 180^\circ$	$\pm 180^\circ$	$\pm 180^\circ$	$\pm 180^\circ$	N.S.	$\pm 180^\circ$	$\pm 180^\circ$	$\pm 180^\circ$
DOF 3: microcatheter translation	Continuous*	Continuous*	101 cm	Continuous*	N.S.	N.S.	N.R.	N.S.	Continuous*
DOF 4: microcatheter rotation	N.S.	N.S.	$\pm 180^\circ$	N.S.	N.S.	N.S.	N.R.	N.S.	$\pm 180^\circ$
DOF 5: guide catheter translation	100 mm	N.S.	800 mm	N.S.	Extended via regripping (SSL 20 mm)	Continuous*	Extended via regripping (SSL N.R.)	300 mm	Continuous*
DOF 6: guide catheter rotation	$\pm 180^\circ$	N.S.	$\pm 180^\circ$	N.S.	$\pm 180^\circ$	$\pm 180^\circ$	$\pm 180^\circ$	$\pm 180^\circ$	$\pm 180^\circ$
Dimension (mm × mm × mm)	N.R.	N.R.	N.R.	180 × 390 × 490 (drive 2 instruments)	190 × 90 × 64 (drive 2 instruments)	238 × 100 × 64 (drive 1 instrument)	1430 × 365 × 305 (drive 3 instruments)	360 × 250 × 250 (drive 2 instruments)	345 × 249 × 115 (drive 3 instruments)
Actuation mechanism	Friction rollers + clamped-wheel rotation	Friction rollers + clamped-wheel rotation	Friction rollers + bionic-finger rotary	Friction rollers + clamp-based linear	Clamp-based linear	Friction rollers + bionic-finger rotary	Clamp-based linear motion + bionic-finger rotary	Friction rollers + clamped-wheel rotation	Friction rollers + clamped-wheel rotation
Manually backdrivable	N.R.	No	N.R.	No	No	No	No	No	Yes
Non-capital equipment	No	Yes	No	No	Yes	N.R.	No	Yes	Yes
Procedure	PCI	PVI	PVI	PCI	N.R.	N.R.	NVI, PCI	PCI	NVI, PCI, PVI
Key limitation	Large footprint; Coupled guidewire T/R	Limited DOFs	Large footprint; Robotic-catheter dependent	Limited DOFs	Limited DOFs; Short SSL	Limited DOFs	Large footprint; Coupled catheter T/R	Coupled guidewire T/R	Haptic feedback not yet implemented

Abbreviations: N.R. = not reported; N.S. = not supported; T/R = translation and rotation; SSL = single-stroke length; PCI = percutaneous coronary intervention; PVI = peripheral vascular intervention; NVI = neurovascular intervention. *Continuous means the DOF range is limited only by the loaded-instrument length.

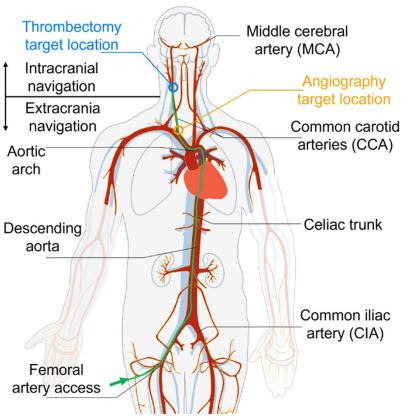

Fig. 1. Our robot targets representative neurovascular workflows from femoral access to extracranial and intracranial vascular targets. The orange and blue markers indicate representative angiography and thrombectomy targets presented in this work, respectively. These workflows motivate a compact, device-agnostic, and reconfigurable robot that actuates off-the-shelf guidewires and catheters and scales from a two-module configuration for diagnostic angiography to a three-module configuration for aspiration thrombectomy.

demonstrated robotic catheter and sheath navigation but depends on proprietary instruments and was limited by system complexity and cost [11]. R-One enables robotic PCI but actuates only a guidewire and a microcatheter with 3 DOFs and remains a largely fixed-base architecture [12]. Recent studies have explored clamp-based, roller-based, and collaborative multimanipulator actuation mechanisms [13], [14], [15], [16] but still trade-off stroke length, mechanical simplicity, procedure-level scalability, or compatibility with standard off-the-shelf devices (see Table I).

Despite recent progress, two major limitations remain in state-of-the-art endovascular robots. First, many existing robots still couple instrument translation and axial rotation or rely on limited-stroke or regrasping mechanisms that slow instrument retraction, which hinder efficient multidevice workflows. In addition, most robots are not truly instrument-agnostic: they support only a limited instrument set within narrow diameter ranges or require customized devices, reducing compatibility across procedures. Second, most platforms remain fixed architectures with limited reconfigurability, making it difficult to adapt the robot across different procedures, scale the number of actuated instruments, or support module-level device exchange. Moreover, most robots are not tailored for neurovascular interventions and do not provide sufficient DOFs for instrument actuations, which can require clinicians to intermittently revert to manual manipulation.

To address the first problem of coupled instrument translation and rotation and limited instrument compatibility, we propose the mechanism design of a decoupled 2-DOF robotic module that *enables independent or simultaneous instrument translation and rotation without causing unwanted resultant force on the instrument*. We further design an instrument-agnostic adjustable clamping mechanism that accommodates off-the-shelf catheters and guidewires with diameters ranging from 0.33 to 3 mm while maintaining reliable traction.

To address the second problem of limited procedural adaptability and time-consuming device exchange, we propose the mechatronic design of a modular robot (see Fig. 2) with interchangeable adapters and reconfigurable multimodule assembly. By swapping adapters, the same module can be configured for guidewire actuation using a torque device or for catheter actuation, with interfaces compatible with standard Luer-lock and Y-connector that provide ports for contrast injection and aspiration. Our modular configuration *supports module-level device exchange by preloading instruments to replaceable modules, thus avoiding instrument reloading into*

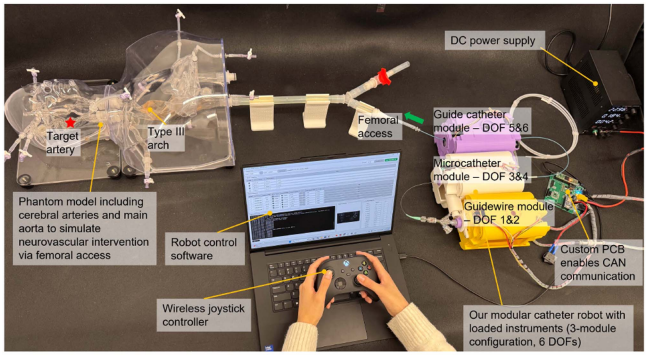

Fig. 2. System overview of proposed LegoBot in a three-module triaxial thrombectomy configuration, which provides 6 DOFs for three commercially available instruments: a guidewire, an intermediate/aspiration catheter, and a guide catheter. Each module contributes one translation DOF and one axial-rotation DOF. The setup also includes a custom printed circuit board (PCB) that enables controller area network (CAN) communication, a wireless joystick, and a host PC running control software.

the robot during the procedure. We also design a module coupler that combines adjacent modules and improves rotational torque transmission through long, compliant instruments.

The contributions of this article include the following.

1) Mechanism design of a decoupled, instrument-agnostic 2-DOF actuation module compatible with off-the-shelf instruments ranging from 0.33 to 3 mm in diameter, which many state-of-the-art systems do not accommodate.
2) Mechatronic design of a robot system consisting of three robotic modules with interchangeable adapters and a dedicated module coupler for reconfigurable neurovascular workflows, such as diagnostic angiography and aspiration thrombectomy.

II. Design Requirements

Our design targets a compact robot that can manipulate standard catheters and guidewires for key neurovascular workflows, including diagnostic angiography and aspiration thrombectomy. These procedures share similar access routes but differ in instrument-stack complexity and coordination: angiography typically requires coordinated advancement and rotation of a guidewire and catheter to reach intracranial targets and deliver contrast, while thrombectomy demands controlled manipulation of a biaxial or triaxial set of instruments to reach distal vasculature and perform clot removal.

To support these tasks, the robot needs to satisfy the following four requirements.

1) *Decoupled 2-DOF actuation:* Each module should provide instrument axial translation and self-axis rotation as distinct mechanical functions so that the two motions can be commanded independently or simultaneously.
2) *Instrument-agnostic actuation:* The mechanism should accommodate guidewires and catheters with outer diameters ranging from 0.33 to 3 mm via adjustable clamping while delivering forces and torques that meet the reported clinical requirements (4.5 N insertion and 8 mN·m rotation [19]).
3) *Modular reconfiguration and fast module-level device exchange:* The system should be reconfigurable across procedures, scale to the required number of instruments and total DOFs, and reduce intraprocedural instrument reloading effort through the preloaded replaceable modules, while preserving compatibility with standard clinical connectors and accessory interfaces.
4) *Reliable rotation transmission for long instruments and multiaxial intervention:* Because rotation can attenuate along long and tortuous paths, the system should preserve rotational authority through module coupling and coordinated actuation across curved segments. Neurovascular procedures usually demand an effective working length of roughly 1200–1500 mm. The robot should also be as compact as possible to reduce the working-length loss associated with the instrument segment that must remain inside the robot for actuation.

III. Mechatronic Design of a Modular Robot for Neurovascular Intervention

A. Mechanism Design for Decoupled Instrument Translation and Rotation With Continuous Range of Motion

A mechanism that actuates an endovascular intervention instrument must provide at least 2-DOF, i.e., linear translation and axial rotation of the loaded instrument. To imitate the skilled clinician's intervention maneuvers, such as "rotate-and-retract" and "spinning," coordinated control of the two DOFs is also needed. This requires the translation and rotation DOFs to be decoupled and to move independently or simultaneously. In this work, decoupled actuation refers to this mechanism-level property. However, many state-of-the-art endovascular robots achieve 2-DOF actuation through coupled mechanisms. As shown in Fig. 3, typically there are two different translation mechanisms, i.e., clamp-based linear motion and friction roller-driven linear motion, and two different rotation mechanisms, i.e., rotating clamped wheel drive and bionic finger-based rotary motion. By combining one mechanism from each DOF with another mechanism from a different DOF, we have a total of four typical mechanisms to achieve 2-DOF instrument actuation. Rail-based insertion often preserves independent rotation, but its translation range is limited by the sliding-rail length, which increases robot size and can require repeated retreat and regripping. For device exchange, this single-stroke-limited reciprocating motion can slow instrument retraction. On the other hand, although the friction roller-based mechanism can enable continuous instrument translation with a theoretically unlimited range of motion, the friction-driven force exerted by the roller clamping can interfere with the rotational torque exerted by the rotary clamping module, *causing coupled translation/rotation motion and unwanted resultant force that can twist the instrument or drive it out of the clamping.*

To address these limitations, we propose a new 2-DOF mechanism design (see Fig. 3, bottom-left). Instead of directly rotating

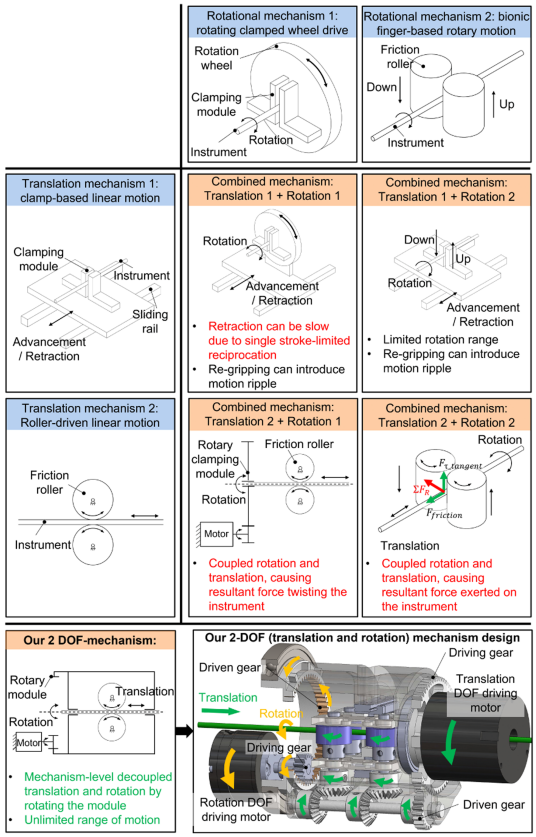

Fig. 3. Comparison of representative 2-DOF actuation mechanisms in state-of-the-art endovascular robots and the proposed mechanism. Top: typical combinations of translation and rotation mechanisms used in existing robots. Bottom-left: the proposed decoupled 2-DOF mechanism design. Bottom-right: computer-aided design (CAD) of our 2-DOF robotic module. Our design enables continuous and decoupled instrument translation and rotation at the mechanism level in a compact cassette form factor that can be used as an interchangeable module across different module configurations.

a gear connected to a separate rotary clamping module, we enclose the entire translational mechanism in a cassette and connect the cassette to a ring gear, forming a rotating cassette module. In this way, the input torque from the rotation motor is applied to the whole translational mechanism rather than directly twisting the instrument through a coupled rotary clamp. Our design preserves a continuous instrument motion range while decoupling translation and rotation at the mechanism level (see Fig. 3, bottom right). The relationship between the motor angles and the instrument translation and rotation is given in the following.

Let ϕ_1 and ϕ_2 (radian) denote the motor angles of motor 1 (insertion) and motor 2 (rotation), respectively. Let (r_1, r_2) be the radii of the driving and driven gears in the insertion drivetrain, (r_3, r_4) be the radii of the driving and driven gears in the rotation drivetrain, and d_R be the diameter of the friction roller. Since all driven bevel gears in the insertion drivetrain share the same gear ratio, the instrument translation x and rotation θ satisfy

$$\theta = s_2\, k_r\, \phi_2 \tag{1}$$

$$x = s_1\, k_t\, \phi_1 \;-\; k_t\, \theta \;=\; s_1\, k_t\, \phi_1 \;-\; s_2\, k_t k_r\, \phi_2 \tag{2}$$

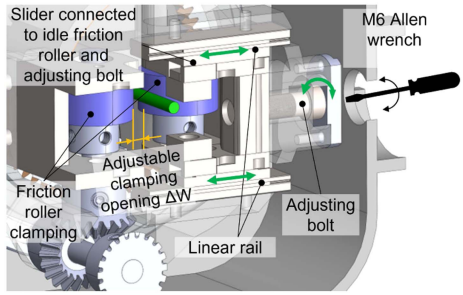

Fig. 4. Adjustable clamping mechanism enabling instrument-agnostic actuation. An adjustable bolt regulates the clamping spacing ΔW to accommodate a wide range of instrument diameters while maintaining consistent traction.

where $k_r = \frac{r_3}{r_4}$, $k_t = \frac{r_1}{r_2}\frac{d_R}{2}$, and $s_1, s_2 \in \{+1, -1\}$ account for the adopted sign convention of motor clockwise/counterclockwise rotation. The cross-term $-s_2 k_t k_r \phi_2$ represents a predictable transmission-level kinematic mapping introduced by the compact drivetrain, where the cassette rotation backdrives the insertion roller and produces an apparent axial motion. This cross-term is compensated via the implemented robot controller. Therefore, the proposed mechanism retains decoupling at the mechanism level, allowing independent or simultaneous translation and rotation actuation without generating undesired resultant forces on the instrument.

B. Design of an Adjustable Clamping Mechanism for Instruments With Different Diameters

State-of-the-art endovascular robots are often compatible with only a small set of catheters/guidewires with limited diameter ranges or require customized devices and dedicated interfaces, which restrict compatibility with off-the-shelf neurovascular instruments (see Table I). To address this limitation, we design an adjustable friction-roller clamping mechanism that accommodates a broad range of commercially available instruments with outer diameters spanning 0.33–3 mm (see Fig. 4). Specifically, the clamping unit employs two opposing roller pairs (four rollers total) to generate axial traction. One side of the roller set is fixed to shafts mounted on the cassette body, while the opposing side is mounted on sliders that translate along linear rails. The slider is mechanically linked to an adjusting screw/bolt that can be threaded in or out using a standard M6 Allen wrench, thereby continuously tuning the roller-to-roller spacing ΔW to match the loaded instrument diameter. This simple manual adjustment provides a wide opening range to accommodate guidewires, microcatheters, intermediate/aspiration catheters, and guide catheters without changing the core actuation hardware.

C. Mechatronic Design of a Modular, Reconfigurable Robot With Interchangeable Adapters for Different Procedures

State-of-the-art endovascular robots are typically built as monolithic hardware platforms with fixed instrument interfaces, making it difficult to reconfigure the system across procedures

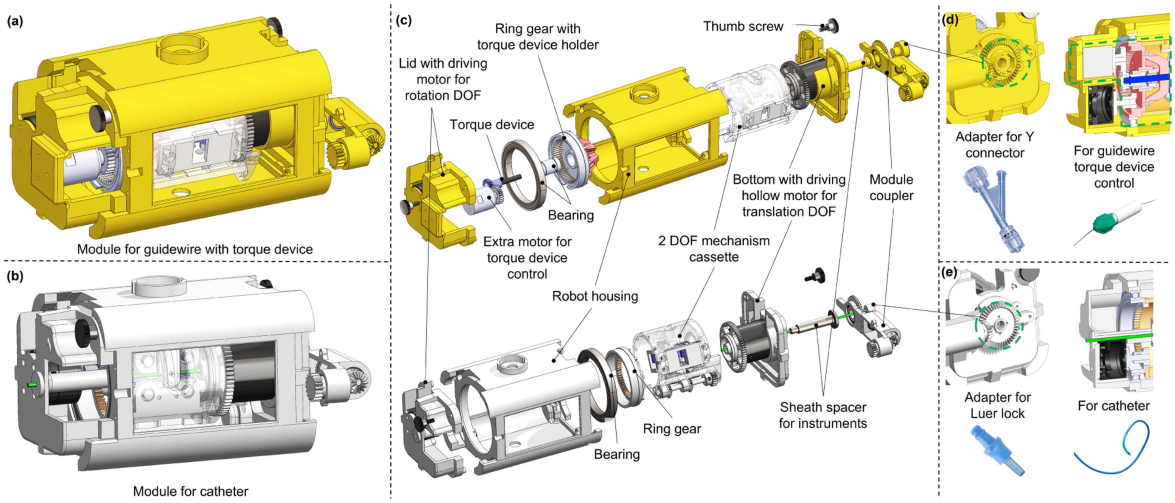

Fig. 5. Mechatronic design of our robotic module. The robot consists of a top lid with the motor for the instrument rotation DOF, a central housing, a 2-DOF mechanism cassette, a bottom lid with the motor for the translation DOF, and a module coupler, together with other components, such as gears, bearings, thumb screws, and instrument-specific sheath spacers. The mechanical interfaces between each part are designed for quick release, enabling rapid attachment and removal of modules and their loaded instruments. By exchanging different adapters, the robot can be configured as (a) a guidewire module with a torque device, or (b) a catheter module. (c) Exploded view of the modular assemblies. (d) Guidewire configuration, including an adapter for a standard hemostatic valve Y-connector (for connection to a contrast syringe or aspiration pump) and an additional motorized mechanism for fastening/releasing the torque device. (e) Catheter configuration, including an adapter for interfacing with a standard Luer-lock connector.

and often requiring full instrument withdrawal and reloading for device exchange. To address this limitation, we propose the design of a modular, reconfigurable endovascular robot in which each building block is a cassette-based 2-DOF module with interchangeable adapters, enabling procedure-specific assembly and module-level rapid device exchange (see Fig. 5). Each module shares a common mechatronic architecture consisting of a 2-DOF mechanism cassette, a motor for translation, a motor for rotation, and standardized mechanical interfaces secured by thumb screws for rapid attachment and removal. By swapping the lid-end adapter, the same module can be configured as 1) a guidewire module that includes an additional small motor to fasten or release the lid of a torque device, thereby switching between guidewire rotation and insertion, or 2) a catheter module. We also designed interchangeable connectors that are compatible with standard clinical interfaces (e.g., Luer-lock adapters and a Y-connector adapter providing a side port for contrast injection or aspiration-pump connection). Each module also incorporates instrument-specific sheath spacers on both sides of the roller set to constrain radial excursion through the drive region. The spacers limit radial displacement while leaving axial translation unobstructed. During long-path driving, downstream bending resistance can induce lateral loading on the instrument. The sheath spacers thus help keep the instrument centered within the roller contact region and reduce the chance of side slip-out. Different spacer openings are used for guidewires, microcatheters, and guide catheters.

This architecture supports module-level device exchange using preloaded replaceable modules. In a triaxial configuration, for example, an inner guidewire can be exchanged while the outer microcatheter and guide catheter remain in place. The guidewire is first retracted until its distal end returns to the outlet side of its own module. That module is then detached and replaced by another module that has already been preloaded with the new guidewire. After reconnecting the microcatheter's Luer connector to the module coupler, the new guidewire is advanced back into the vasculature. This workflow eliminates the time-consuming bare-instrument reloading into the actuation mechanism during exchange. Assembling three modules yields a compact 6-DOF system (see Fig. 6) for neurovascular triaxial workflows involving a guidewire, a microcatheter/working catheter, and a guide catheter, with an overall size of $345 \times 249 \times 115\ \text{mm}^3$, which is about 50% smaller than our previous robot design [16]. Relative to that prior robot, the present system also introduces a new mechanism-level decoupled 2-DOF module, a new clamping mechanism, a fully modular architecture enabling module-level exchange, and a dedicated module coupler.

D. Design of the Module Coupler to Enhance Rotational Torque Transmission

Long, slender endovascular instruments (e.g., guidewires and microcatheters) often exhibit torsional compliance and frictional stick–slip along their extended length and through tortuous paths, such that proximal rotation applied by the robot may be absorbed by shaft twist and friction before reaching the distal end. To mitigate this effect while enabling modular assembly, we design a dedicated module coupler (see Fig. 7) with two functions: 1) mechanically connecting adjacent 2-DOF modules to form procedure-specific 6-DOF/8-DOF configurations, and 2) providing additional distal-side torque input to improve rotational torque transmission through long, compliant instruments. Specifically, the coupler incorporates an input spur gear that also meshes with the ring gear in the rotation drivetrain. When the rotation motor actuates the ring gear, the spur gear drives

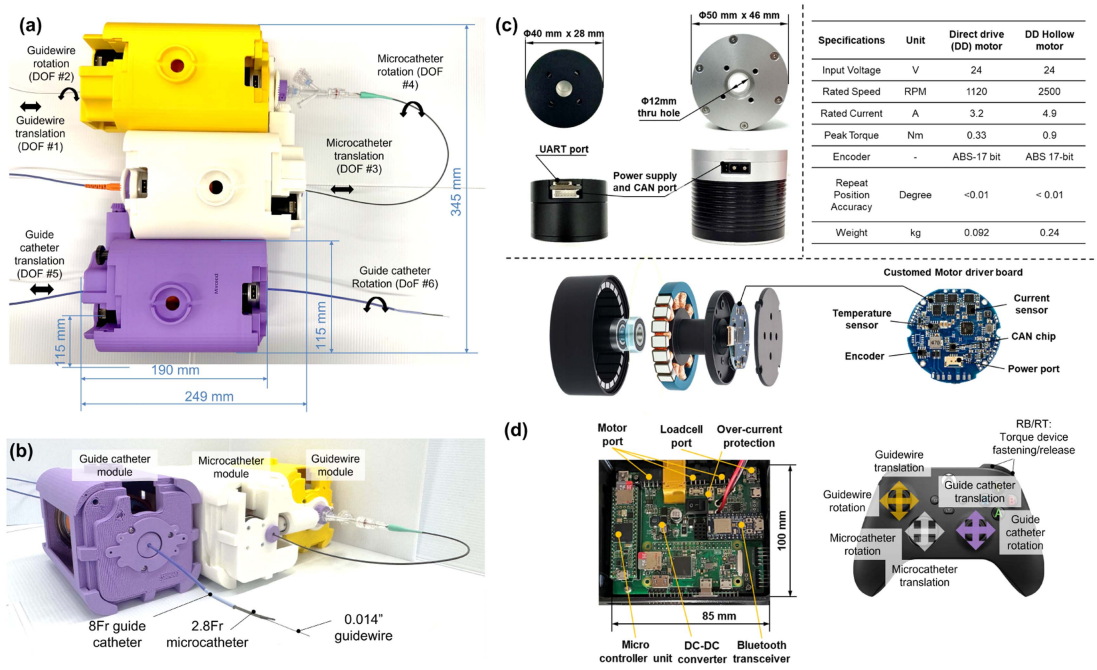

Specifications	Unit	Direct drive (DD) motor	DD Hollow motor
Input Voltage	V	24	24
Rated Speed	RPM	1120	2500
Rated Current	A	3.2	4.9
Peak Torque	Nm	0.33	0.9
Encoder	-	ABS-17 bit	ABS 17-bit
Repeat Position Accuracy	Degree	<0.01	< 0.01
Weight	kg	0.092	0.24

Fig. 6. (a) and (b) Prototype of our 6-DOF robot incorporating a 2-DOF guide catheter module, a 2-DOF microcatheter/working catheter module, and a 2-DOF guidewire module. (c) Two custom direct-drive brushless DC (BLDC) motors provide compact high-torque density actuation with integrated sensing and facilitate hand backdrivability, allowing manual override in an emergency. (d) Our custom PCB supports motor communication and system control through a microcontroller unit, CAN communication, power electronics, and Bluetooth.

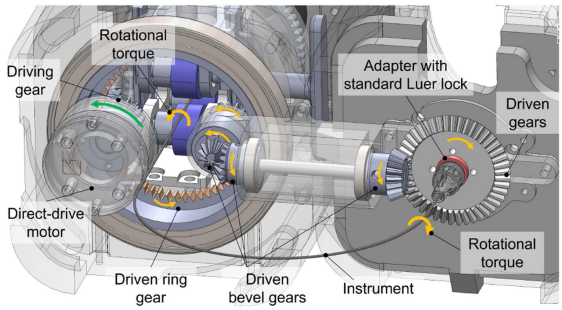

Fig. 7. Proposed coupler mechanically links adjacent modules and couples to the rotation drivetrain: an input spur gear meshes with the ring gear, driving a bevel gear that delivers additional torque to the distal-side connector, enabling two-end torque actuation to improve rotational torque delivery through curved, compliant instruments. Without the coupler, proximal rotation applied at the robot side can be attenuated by torsional compliance and friction along the guidewires or microcatheters.

a bevel-gear-and-shaft transmission that applies an additional compensatory torque to the connector, opposite in direction to the cassette-side torque. The resulting two-end torque actuation is designed to improve effective torque delivery through curved and compliant instruments.

E. Electronics for Communication and Control

The electronics architecture integrates compact direct-drive motors with a custom-designed PCB for real-time communication and teleoperation control. Our PCB powers a Teensy 4.1 (PJRC) microcontroller and communicates with the motors through a 1 Mbps CAN bus. The firmware executes a deterministic 500-Hz command pipeline to the motors with a 200-Hz uplink to the host PC. User commands are issued from an Xbox controller to the host PC, providing access to live telemetry and control parameters, and forwarded to the firmware. We custom made two highly integrated BLDC electric motors (GYEMS Co., Ltd.), featuring built-in motor drivers, dual 17-bit magnetic encoders, and current sensors within a compact form factor. The first motor (ϕ 40 mm $\times$ 28 mm) delivers a peak torque of 0.33 N·m with a torque density of 3.67 N·m/kg and speeds up to 1120 r/min, which drives instrument translation and coordinated push–pull motion. The second motor (ϕ 50 mm $\times$ 46 mm) has a ϕ 12 mm central aperture to facilitate catheter passage, thus simplifying the mechanism design. The hollow motor delivers a peak torque of 0.9 N·m (3.75 N·m/kg) to drive instrument rotation. By utilizing a gearless design, these actuators eliminate mechanical backlash and the bulky footprint associated with gearboxes and facilitate hand backdrivability. To ensure operational safety, the system implements motor current limiting, physical and graphical user interface (GUI) emergency stops, communication quality monitoring for packet jitter and loss, a 10 Hz displacement continuity check to prevent operation under degraded communication, and a 2-Hz watchdog for thread and input/output (I/O) deadlock prevention. The present prototype relies on motor-side sensing for actuation monitoring, while direct sensing of true instrument motion is not yet included in this version.

IV. Experiments and Results

We evaluated the proposed robot through benchtop characterization and phantom demonstrations of representative neurovascular intervention for stroke treatment. The benchtop

tests quantified the force and torque capability of the 2-DOF module, the achievable insertion force across five off-the-shelf instruments, and qualitative behaviors directly relevant to the proposed mechanism and modular architecture, including compensation-enabled actuation, module-level device exchange, coupler-assisted rotation transmission, and visual inspection for instrument integrity. The phantom studies evaluated representative neurovascular workflows enabled by two-module and three-module robot configurations.

A. Benchtop Characterization of the Robotic Module

1) Validate Maximum Insertion Force and Rotational Torque of 2-DOF Robotic Module: To validate the insertion force and rotational torque capacity of the proposed 2-DOF mechanism, we developed a benchtop testbed using 3D-printed fixtures, a load cell, and a supporting sheath to prevent buckling of the instrument segment outside the robot. An 8 Fr guide catheter was loaded into the robot module for both insertion force and rotational torque tests. For maximum insertion force measurement, the catheter was advanced by the friction rollers to push against a rigid vertical wall connected to the load cell [see Fig. 8(a)]. The peak insertion force was measured as the load-cell reading immediately before traction loss. For rotational-torque measurement, the same catheter was connected to a reel-wire-load-cell setup [see Fig. 8(b)], and the torque was computed as $\tau_r = F_p \times r$, where $r = 5$ mm is the reel radius. As shown in Fig. 8(c) and (d), the measured peak insertion force reached 5.3 N and the measured peak rotational torque reached 8.4 mN·m, both exceeding the reported clinical requirements of 4.5 N and 8 mN·m, respectively.

2) Validate Capability of the Proposed Clamping Mechanism to Drive Off-the-Shelf Instruments: To validate the proposed clamping mechanism's capability to accommodate and actuate off-the-shelf instruments for neurovascular interventions, we measured the maximum insertion force achievable before buckling for five commercially available off-the-shelf instruments in the three-module setup [see Fig. 8(e)]. Using the same load cell and 3D-printed fixture as in the previous insertion-force test, except that the instrument was advanced through a simulated aortic support path before contacting the rigid wall, we recorded the peak force at the onset of instrument buckling. The measured peak forces were 0.1 N for a 0.014-inch guidewire (ACUITY Whisper View Guidewire with Hydrophilic Coating, Straight Tip, Boston Scientific), 0.48 N for a 0.028-inch microcatheter (MAMBA Flex Microcatheter, Boston Scientific), 0.31 N for a 2.8 Fr microcatheter (Direxion HI-FLO Microcatheter, J Shape, Boston Scientific), 0.39 N for a 5 Fr angiographic catheter (Accu-Vu Angiographic Sizing Catheter, Non-Braided, Angio-Dynamics), and 4.3 N for an 8 Fr guide catheter (Launcher Guiding Catheter, Medtronic) [see Fig. 8(f)–(i)]. The peak forces were not strictly proportional to instrument diameter because buckling also depended on shaft stiffness, jacket construction, and tip geometry. These results support the ability of the proposed adjustable clamping mechanism to accommodate and actuate off-the-shelf instruments with different diameters and mechanical properties.

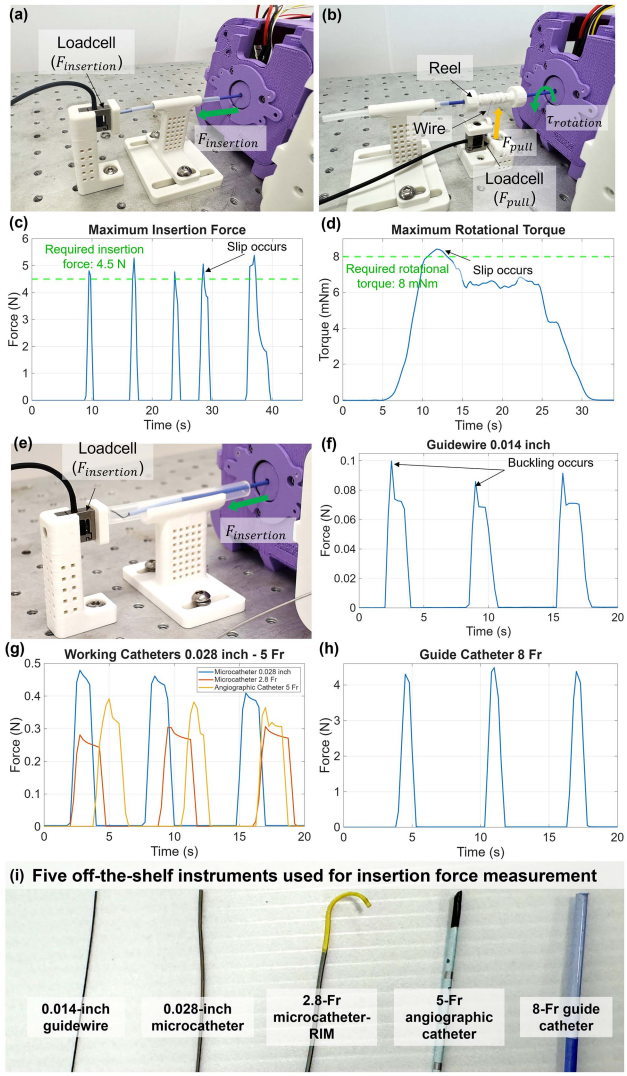

Fig. 8. Benchtop characterization of the proposed module. (a) Maximum insertion-force test setup. (b) Maximum rotational-torque test setup. (c) Maximum insertion force measurements up to slip. (d) Maximum rotational torque measurement up to slip. (e) Testbed for maximum insertion force before buckling in a simulated vascular path. (f)–(i) Peak insertion force measured across five off-the-shelf instruments with different diameters and stiffnesses.

3) Qualitative Validation of Kinematic Compensation, Module Exchange, and Coupler Mechanism: We conducted three additional benchtop validations to directly examine the mechanism and workflow claims of the proposed system. In a single-module test with a marked catheter, we first evaluated the implemented transmission compensation. When the compensation was disabled, a rotation command induced coupled insertion and independent rotation was not attainable. When the compensation was enabled, the same module supported rotation-only, translation-only, and simultaneous translation–rotation actuation. We then evaluated module-level exchange in a coaxial guidewire–angiographic-catheter configuration, where replacement of a preloaded angiographic-catheter module required 1 min 50 s in a representative timed trial. To assess the dedicated coupler, we performed a single-module comparison

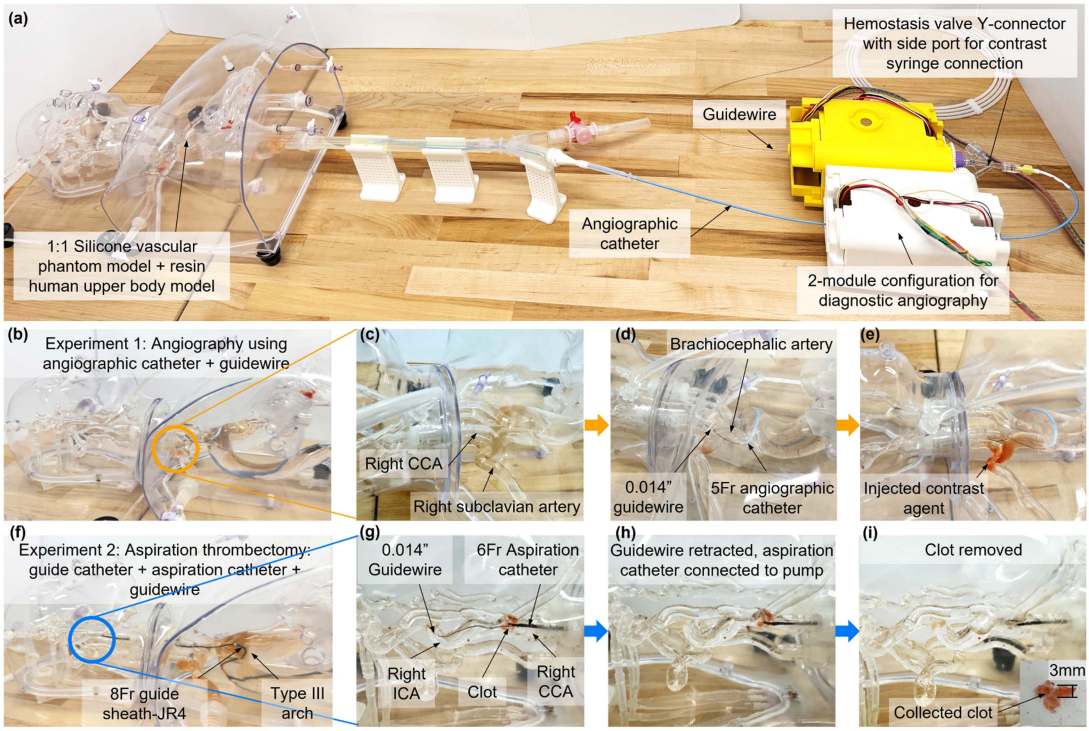

Fig. 9. Phantom experiments of representative neurovascular workflows enabled by the proposed modular robot. (a) Two-module robot configuration (Three-module configuration is shown in Fig. 2). (b)–(e) Diagnostic angiography with a two-module (4-DOF) setup actuating a guidewire and an angiographic catheter, including contrast injection through a standard Y-connector. (f)–(i) Aspiration thrombectomy with a three-module (6-DOF) setup actuating a guide catheter, an aspiration catheter, and a guidewire, including clot aspiration through a standard clinical interface.

using a marked microcatheter. With the coupler engaged, the microcatheter completed five full rotations, whereas without the coupler the visible transmitted rotation was limited to about 180° before torsional slip-back. These qualitative results are provided in the Video in the Supplementary Material.

B. Phantom Experiments of Neurovascular Procedures

1) Diagnostic Angiography With Two Modules Driving Angiographic Catheter and Guidewire: We first conducted in vitro diagnostic angiography in a silicone neurovascular phantom, including a femoral access inlet, a Type III aortic arch, and supra-aortic branches [see Fig. 9(a) and (b)]. A two-module (4-DOF) robot configuration actuated a 0.014-inch guidewire and a 5 Fr angiographic catheter introduced from the femoral access. The guidewire was robotically advanced through the Type III arch into the brachiocephalic trunk and then into the right common carotid artery (CCA), after which the angiographic catheter was advanced over the guidewire to the same target region [see Fig. 9(d)]. The angiographic catheter interfaced with a standard hemostatic valve/Y-connector assembly, through whose side port contrast was manually injected to visualize the target branch [see Fig. 9(e)].

2) Aspiration Thrombectomy With Three Modules Driving Guide Catheter, Aspiration Catheter, and Guidewire: We also performed aspiration thrombectomy in the same phantom using a three-module (6-DOF) configuration to actuate an 8 Fr guide catheter, a 6 Fr aspiration catheter, and a 0.014-inch guidewire [see Fig. 9(f)]. A clot analog was placed near the right CCA–internal carotid artery (ICA) region to create an occlusion. The guidewire and guide catheter were first navigated to establish access, after which the guidewire crossed the occlusion, and the aspiration catheter was advanced to the clot face [see Fig. 9(g)]. The clot was then retrieved by aspiration through a portable vacuum pump manually connected to the Y-connector after guidewire retraction [see Fig. 9(h) and (i)]. Throughout the robotic navigation and clot-removal procedure, no side slip-out from the roller contact region was observed with the sheath spacers installed. All instrument navigation and positioning were robotically performed; the only manual actions were contrast or aspiration connection through standard clinical interfaces.

V. Discussion and Conclusion

In this work, we presented LegoBot, a compact modular catheter robot composed of interchangeable 2-DOF modules that provide mechanism-level decoupled translation and rotation together with instrument-agnostic actuation of off-the-shelf devices. Benchtop characterization showed peak insertion force up to 5.3 N and rotational torque up to 8.4 mN·m, while additional qualitative validations further supported compensation-enabled actuation to achieve independent and simultaneous rotation and translation, module-level fast device exchange, and coupler-assisted rotation transmission. Phantom studies further demonstrated representative neurovascular workflows using a two-module configuration for diagnostic angiography and a three-module configuration for aspiration thrombectomy. These

results support LegoBot as a compact and reconfigurable platform for multi-instrument neurovascular intervention. The proposed mechanism is decoupled at the mechanism level, while the residual transmission-level kinematic cross-term is predictable and compensated in command. The main limitation of the present prototype is that it relies on motor-side sensing and does not directly measure true instrument motion under slip or compliance. Although our prior work using a friction-roller-based actuation mechanism reported task-space tracking using motion capture and electromagnetic sensing [16], quantitative distal tracking of the present modular system remains future work. Force/haptic feedback, sterile-workflow validation, blood-flow effects, and in vivo evaluation are outside the scope of this study but will be explored in future work. Overall, our robot provides a practical mechatronic basis for future translational development of modular endovascular robots.

V. Acknowledgment

ChatGPT was used during the preparation of this manuscript to refine the writing after the authors completed the initial draft.

References

[1] A. Duclos et al., "Safety of inpatient care in surgical settings: Cohort study," *BMJ*, vol. 387, 2024, Art. no. e080480.

[2] H. Su et al., "An MRI-guided concentric tube continuum robot with piezoelectric actuation: A feasibility study," in *Proc. IEEE Int. Conf. Robot. Autom.*, 2012, pp. 1939–1945.

[3] H. Su et al., "State of the art and future opportunities in MRI-guided robot-assisted surgery and interventions," in *Proc. IEEE*, vol. 110, no. 7, pp. 968–992, Jul. 2022.

[4] C. S. Weyland et al., "Occupational radiation exposure of neurointerventionalists during endovascular stroke treatment," *Eur. J. Radiol.*, vol. 164, 2023, Art. no. 110882.

[5] J. Chakravartti and S. V. Rao, "Robotic assisted percutaneous coronary intervention: Hype or hope," *J. Amer. Heart Assoc.*, vol. 8, no. 13, 2019, Art. no. e012743.

[6] N. Kaneko, C. Beaman, T. Imahori, A. Takayanagi, H. Saber, and S. Tateshima, "In vitro comparison of manual and robotic endovascular thrombectomy for acute ischemic stroke," in *Interventional Neuroradiology*, 2023, Art. no. 15910199231206315.

[7] X. Bao et al., "Multilevel operation strategy of a vascular interventional robot system for surgical safety in teleoperation," *IEEE Trans. Robot.*, vol. 38, no. 4, pp. 2238–2250, Aug. 2022.

[8] C. Beaman, N. Kaneko, P. Meyers, and S. Tateshima, "A review of robotic interventional neuroradiology," *Amer. J. Neuroradiol.*, vol. 42, no. 5, pp. 808–814, 2021.

[9] V. Vidal, I. Bargellini, C. Bent, S. Kee, M. Little, and G. O'Sullivan, "Performance evaluation of a miniature and disposable endovascular robotic device," *CardioVascular Interventional Radiol.*, vol. 47, no. 4, pp. 503–507, 2024.

[10] O. Moschovaki-Zeiger, N.-A. Arkoudis, and S. Spiliopoulos, "Safety and feasibility study of a novel robotic system in an in vivo porcine vascular model," *CVIR Endovascular*, vol. 7, no. 1, 2024, Art. no. 14.

[11] W. Crinnion et al., "Robotics in neurointerventional surgery: A systematic review of the literature," *J. Neurointerventional Surg.*, vol. 14, no. 6, pp. 539–545, 2022.

[12] E. Durand, R. Sabatier, P. C. Smits, S. Verheye, B. Pereira, and J. Fajadet, "Evaluation of the R-One robotic system for percutaneous coronary intervention: The R-EVOLUTION study," *EuroIntervention*, vol. 18, no. 16, 2023, Art. no. e1339.

[13] M. E. Abdelaziz et al., "Toward a versatile robotic platform for fluoroscopy and MRI-guided endovascular interventions: A pre-clinical study," in *Proc. IEEE/RSJ Int. Conf. Intell. Robots Syst.*, 2019, pp. 5411–5418.

[14] H. Baek, B. Cheon, J. M. You, and D.-S. Kwon, "Design and analysis of feeder mechanism for buckling prevention in robotic catheterization," *J. Comput. Des. Eng.*, vol. 9, no. 4, pp. 1467–1481, 2022.

[15] S. Cao et al., "A reciprocating delivery device-based endovascular intervention robot with multimanipulators collaboration," *IEEE Trans. Instrum. Meas.*, vol. 73, 2023.

[16] N. T. Kantu, W. Gao, N. Srinivasan, G. D. Buckner, and H. Su, "Portable and versatile catheter robot for image-guided cardiovascular interventions," *IEEE/ASME Trans. Mechatron.*, vol. 30, no. 6, pp. 7985–7994, Dec. 2025.

[17] V. M. Pereira et al., "First-in-human, robotic-assisted neuroendovascular intervention," *J. Neurointerventional Surg.*, vol. 12, no. 4, pp. 338–340, 2020.

[18] A. K. Ghamraoui and J. J. Ricotta, "Current and future perspectives in robotic endovascular surgery," *Curr. Surg. Rep.*, vol. 6, no. 12, 2018, Art. no. 21.

[19] D. Ilić, "Haptic instrumentation for an interventional radiology simulator," Ph.D. dissertation, École Polytechnique Fédérale de Lausanne (EPFL), Lausanne, Switzerland, 2005.